Large-Scale Aspects of Deep Convective Activity over the GATE Area

MASATO MURAKAMI[1]

Department of Meteorology, Florida State University, Tallahassee 32306

(Manuscript received 19 May 1978, in final form 16 April 1979)

ABSTRACT

Using digital IR data obtained by SMS 1 satellite, the large-scale behavior of convective activity was investigated over the tropical Atlantic within the GATE area. Spectral analysis has revealed the existence of two remarkable periodicities which show good association with the large-scale atmospheric field, namely, a 4–5 day mode and a diurnal mode.

The area of the enhanced convection associated with the 4–5 day mode moves westward from Africa through the tropical Atlantic. Its mean phase speed turned out to be about 7° day^{-1} and the mean wavelength about 30° in longitude. The vertical structure of the corresponding disturbance was investigated by the time-composite technique applied to upper air data over the GATE A/B area. The result shows that the enhancement of convection is associated with deep upward motion throughout the troposphere and southerly (northerly) winds in the lower (upper) troposphere. It also shows that the enhancement is accompanied by moistening in the cloud layer, while drying appears in the subcloud layer.

As for the diurnal mode, composited variation shows the maximum convective activity in the late afternoon over the GATE A/B area. Horizontal distributions of the composited anomalies revealed that the late afternoon maxima have a zonal distribution roughly along 10°N rather than the confined one in the vicinity of West Africa. It also revealed the coexistence of the region which shows the early morning maximum. The latter takes place to the south of the former one over the middle Atlantic.

Diurnal components of the large-scale kinematic and thermal fields were also examined over the A/B area. During the daytime, the vertical motion shows upward anomalies and the temperature shows distinct warm anomalies in the upper troposphere. As for the moisture variation, the atmosphere tends to show dry anomalies near local noon and moist anomalies near midnight.

1. Introduction

The large-scale controlling effect on cumulus convective activity has long been recognized as a crucial element in tropical meteorology. Past achievement in theoretical and numerical works which used convective parameterization has clearly demonstrated this importance. In fact, the understanding of the scale interaction between convective activity and large-scale weather systems was one of the central objectives of the GARP Atlantic Tropical Experiment (GATE) which was conducted in 1974.

In the field of data analysis, the improvement of satelliteborne observation in the past two decades has enabled us to grasp the large-scale organization of convective activity. Its usefulness in dealing with such convective systems was demonstrated by Chang (1970), who made longitude-time diagrams from satellite photographs and showed the systematic behavior of large-scale cloud patterns. The launch of a geosynchronous satellite and the measurement of infrared brightness have further improved the situation by providing nearly continuous data over a wide area in the tropics.

GATE has provided an excellent opportunity in the sense that it combined both satellite and dense upper air observations over the tropical Atlantic and West Africa where data are normally very sparse. Since this experiment was carried out, a number of investigations have been performed which utilized such data sets. For example, Reed *et al.* (1977) investigated the structure of the synoptic-scale disturbance which travels westward from West Africa through the eastern Atlantic. They noted that it controls the convective activity in such a way that the maximum activity takes place ahead of the trough.

Analyses of GATE data sets have also shown evidence of the diurnal control of large-scale convective activity. Gruber (1976) examined satellite-observed cloudiness over the GATE A/B area and showed that it reaches a maximum in the afternoon, somewhat in contradiction to previous results over other oceanic areas. McGarry and Reed (1978) intensively investigated the diurnal variation in convective activity over West Africa and the adjacent eastern Atlantic. They showed that the enhanced

[1] Present affiliation: Meteorological Research Institute, Tokyo 166, Japan.

0027-0644/79/080994-20$09.00

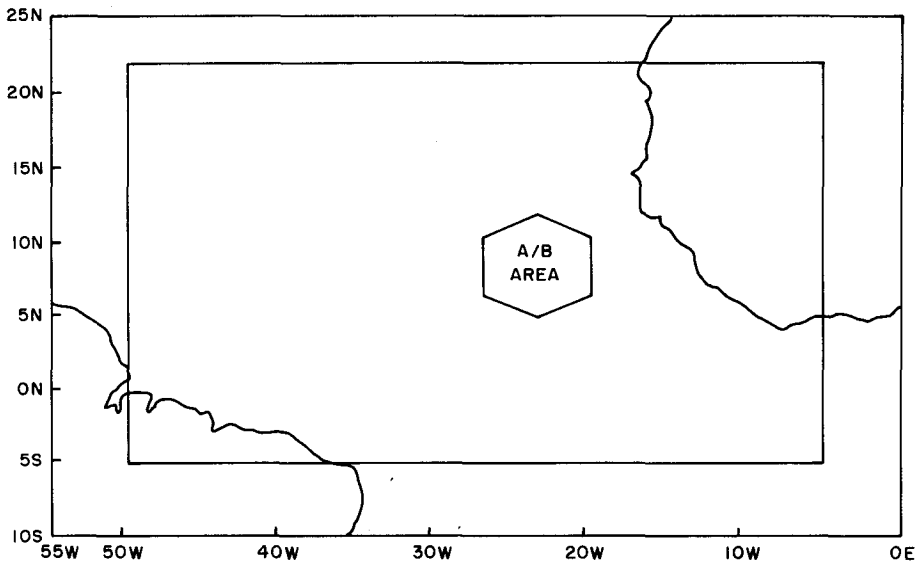

FIG. 1. Area of analysis. The rectangle in the map represents the area over which IR data are analyzed, hexagon is the perimeter of the A/B area.

activity in convective clouds occurs near midnight over land, and in the early afternoon over the adjacent ocean. In addition, they also found that there is a considerable fluctuation in phase and amplitude of the diurnal variation over the ocean. This aspect has been one of our major concerns in the present study.

The purpose of this study is to investigate the temporal and spatial behavior of large-scale convective activity over the tropical Atlantic and to see in what manner it is organized in the large-scale sense. It is also our interest to see the association with the large-scale atmospheric field. In order to accomplish these purposes, we have tried to take advantage of satellite observations during the GATE period as fas as possible. Since there is evidence of the coexistence of different time scales in the variation of convective activity, we have employed the technique of time-series analysis as a tool for a systematic approach. In Section 3 we shall see that more than one characteristic time scale can be specified in that manner. In Section 4 we deal with the characteristic behavior of each mode, and the associated variation in the large-scale atmospheric fields will be discussed in Section 5.

2. Data

Digital infrared (IR) data observed by the Synchronous Meteorological Satellite (SMS 1) are chosen to measure the deep convective activity over the GATE area. These digital data have a definite advantage compared with photographic images. Although many investigators have found IR photographs useful in estimating the presence of convective activity (Payne and McGarry, 1977; McGarry and Reed, 1978), they have occasionally been limited by problems which are inherent in photography. One of them comes from the subjective manner in which deep convective activity is distinguished from low or layered clouds. Moreover, photographs are vulnerable to artificial distortion due to overexposure. Digital data can distinguish high-top clouds more objectively and they also make it possible in principle to pick up the deep cloud beneath the cirrus canopy by closely examining the digital values and by taking difference of emissivity into account.

Smith and Vonder Haar (1976) have edited the original tapes of the SMS 1 observations over the GATE area, and have produced hourly IR and visible data for the period from 27 June through 20 September 1974. Their resolution was 4 n mi by 4 n mi for IR brightness. In this study, IR data were further edited in such a way that they yield 3 h IR values averaged for each 1° by 1° mesh over the GATE area shown in Fig. 1. After the removal of instrumental drift in the observed values by using the program kindly provided by Dr. Eric A. Smith of Colorado State University, the IR data were classified into 16 counts (0–15) according to the digitized intensity of IR radiance. Note that IR counts in this data set have been reversed with respect to the actual IR irradiance, i.e., higher IR counts correspond to colder equivalent blackbody temperatures. Roughly speaking, count 0 corresponds to more than 50°C in blackbody temperature and count 15 to less than −100°C. A difference of one count is roughly equivalent to a difference of 8°C.

The agreement between the edited IR variation and that of convective activity was examined by

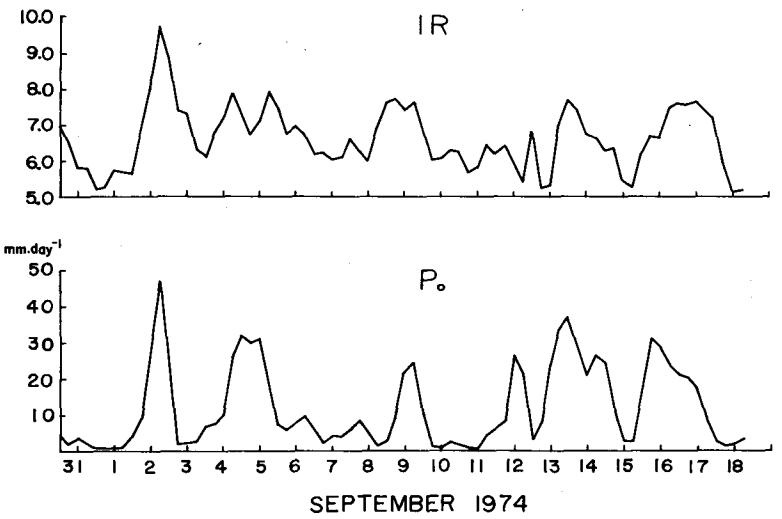

FIG. 2. Comparison between the variations of IR and rainfall intensity (P_0). IR values have been averaged over the A/B area. The variation of P_0 was depicted after Thompson *et al.* (1979).

comparing IR with the rainfall intensity. Recently, Thompson *et al.* (1979) edited the variation of the rainfall intensity over the so-called B-scale area (inner portion of A/B area). Fig. 2 shows the comparison between their time series and the IR variation over the A/B area to which we applied time-series analysis in this study. Despite the different size of the averaged area, one can still see good agreement between these two variables. Since most of the rainfall over this region is supposedly of convective origin, it would be fairly safe to regard the IR variation as the measure of deep convective activity which can produce such a rainfall.

Upper air observations have been rearranged from the GATE Quick Look Data Set for about 13 ships located within the A/B area shown in Fig. 1. Rearrangement was performed in such a way that it produced vertically interpolated data at 25 mb intervals from 100 through 1000 mb and at 6 h intervals starting at 0000 GMT. Vertical interpolation was carried out using a cubic spline technique. After this procedure, the least-square linear-plane fitting was applied to the A/B area so that the horizontal distribution of each meteorological quantity was approximated in the form of $ax + by + c$, where x and y denote eastward and northward directions, respectively. The origin of the coordinate was assigned to the center of A/B array (8.5°N, 23.5°W). Large-scale divergence and vorticity were calculated by using the obtained gradients of the u and v component winds. Large-scale vertical motion was calculated kinematically in terms of p-velocity ω, under the constraint of the mass balance between the surface and 100 mb level following the algorithm proposed by O'Brien (1970).

3. Mean field and temporal variation

Fig. 3 shows the horizontal distribution of the mean IR data averaged over the period from 27 June through 20 September 1974 which includes all three phases of GATE. In general, high IR counts correspond to low temperature at cloud top, thus indicating that there exist many high-top clouds in that area. As illustrated in Fig. 2, this situation can be taken as the manifestation of high convective activity. In Fig. 3 we can see the apparently zonal distribution of high IR counts extending from West Africa through the eastern Atlantic. The axis of maximum values lies between 5 and 10°N over the Atlantic and shows northward displacement when it crosses the coast of West Africa into the inland area. Longitudinally, the IR count reaches its maximum at the coast of West Africa and tends to decrease toward the middle Atlantic.

Latitudinal location of high IR counts over the Atlantic agrees well with the climatological mean position during the summer which was discussed by Gruber (1972) and Gray and Oort (1974) using satellite visible brightness data. It also agrees with the one discussed by Sadler (1975) in terms of the cloudiness obtained from satellite imagery. However, over West Africa the maximum IR count tends to appear to the north of maximum visible brightness or maximum cloudiness. This discrepancy seems to be due to the fact that many of the clouds along the Gulf of Guinea, south of 10°N, are stratiform type rather than deep convective clouds (Carlson, 1969a). Carlson (1969a,b) has also pointed out that disturbances often show their maximum intensity when they reach the coastal region from

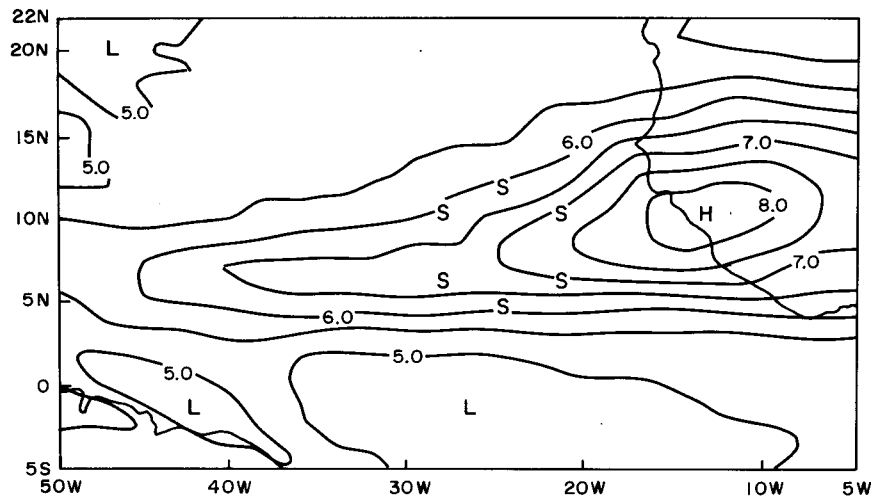

FIG. 3. Horizontal distribution of the mean IR values. S's denote the scheduled positions of GATE A/B ships.

the inland area and tend to decay toward the middle Atlantic. This aspect seems to be reflected in the distribution of mean IR counts which show maximum value over the coast of West Africa.

In order to see the temporal variation of large-scale convective activity, we first examined the variation of IR counts averaged over the A/B area. Fig. 4 exhibits the resultant time series. The time-mean value and the linear trend have been removed in this diagram. Glancing at the diagram, one could get the impression that there exists a kind of quasi-periodic oscillation. It appears that there is a superposition of two different periodicities at least, one an apparently diurnal mode and another which shows an interval ranging from 3 to 5 days or so. These periodicities will be discussed more quantitatively in a later part of this section.

Prior to statistical processing, we look into the longitudinal variation along the parallel of latitude in conjunction with the temporal variation. Fig. 5 presents the longitude-time section of IR counts averaged over the latitude belt from 5 to 10°N which includes the major part of high IR counts shown in Fig. 3. Zonal means are subtracted at each time and the contours are drawn for positive anomalies which supposedly indicate the enhancement of deep convective activity. Negative anomalies are just shaded in this diagram. Although the original diagram was made for the whole period of GATE, only its portion corresponding to Phase II (28 July–16 August) is shown in this paper as an example.

Fig. 5 exhibits the definite existence of the traveling character in the longitudinal eddy part of the IR variation. Most of the enhanced anomalies appear first at the eastern end of the diagram (5°W) and tend to move westward. The enhancement appears widespread to the east of 20°W and shrinks westward, although some of them (e.g., the one around Day 220) show the development in the middle of the Atlantic. The time interval of the passage of major enhanced areas range from about 3 to 5 days over the A/B area which extends from 20°W through

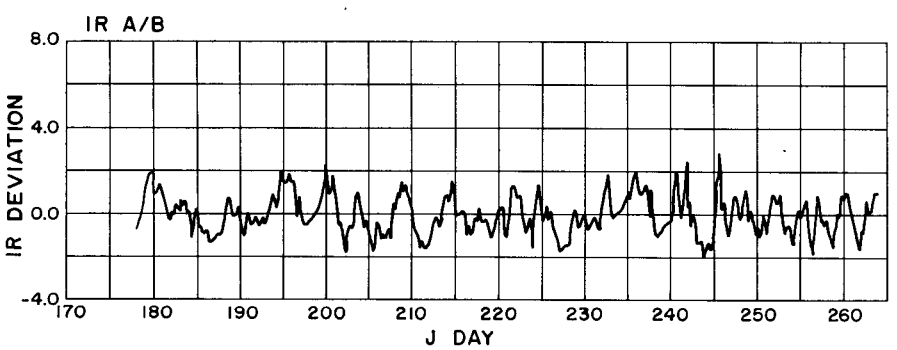

FIG. 4. Time sequence of IR averaged over A/B area. The time mean value has been subtracted and the abscissa denotes the day of the year.

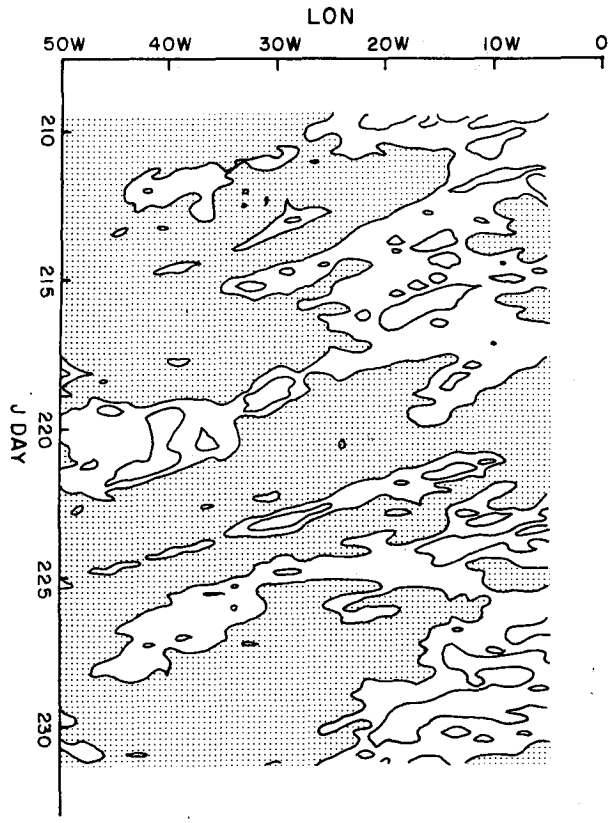

FIG. 5. Longitude-time diagram of IR averaged over latitudes from 5 to 10°N. Zonal means are subtracted and contours are drawn at every 2.0 intervals for positive anomalies. Negative anomalies are stippled. Ordinate denotes the day of the year. Day 210 corresponds to 29 July.

27°W. Although figures are not shown in this paper, the other phases of GATE show similar situations.

In order to specify the above-mentioned periodicities more objectively, a statistical method of spectral analysis was applied to the time series exhibited in Fig. 4. The resultant spectrum is shown in Fig. 6. This figure presents the values of (frequency) × (power spectral density) as a function of log frequency. The advantage of this representation was discussed by Zangvil (1975, 1977). One can see that the spectral distribution shows three major peaks, namely, the peak around a 4–5 day period, that around a 2.5-day period, and the diurnal peak. Among them the 4–5 day peak appears most intense and seems to reflect the major quasi-periodicity which can be seen in Fig. 4 or Fig. 5. This periodicity also coincides with that reported by Burpee (1972, 1974) and others in conjunction with the so-called African waves.

The peak around 2.5 days is of lesser intensity. This short-term periodicity has also been detected in the variations of other meteorological quantities, though its appearance is not necessarily prominent. Murakami (1972) analyzed a 2–3 day mode over the Marshall Islands, and Orlanski (1976) exhibited the results of spectral analyses over the GATE area which show the peak around a 2-day period. Recently Orlanski and Polinsky (1977) analyzed the variation of cloud coverage over Africa and also found the existence of a 2-day mode. They discussed that this mode shows a medium-scale feature rather than a large-scale one.

A diurnal peak in the spectrum is one of the most widely detected features. Gray and Jacobson (1977) discussed the observational evidence which shows the existence of a diurnal cycle in convection over the tropical ocean. Their paper also includes a comprehensive review of past investigations. Gruber (1976) analyzed the cloudiness obtained from the SMS 1 IR imagery over the A/B area and showed the diurnal cycle in the variation of the upper cloudiness. Since the digital IR brightnesses are apt to respond more to the variation of high-top clouds, his finding supports the reality of the diurnal peak in Fig. 6. Recently McGarry and Reed (1978) also analyzed the SMS 1 IR images over the A/B area and West Africa. They discussed the systematic appearance of the diurnal cycle and its relationship with precipitation.

If periodicities in IR data are associated with large-scale changes in the atmosphere, it is natural to expect that the same periodicities can be detected in the time series of those quantities. The investigation of this subject was carried out by applying spectral

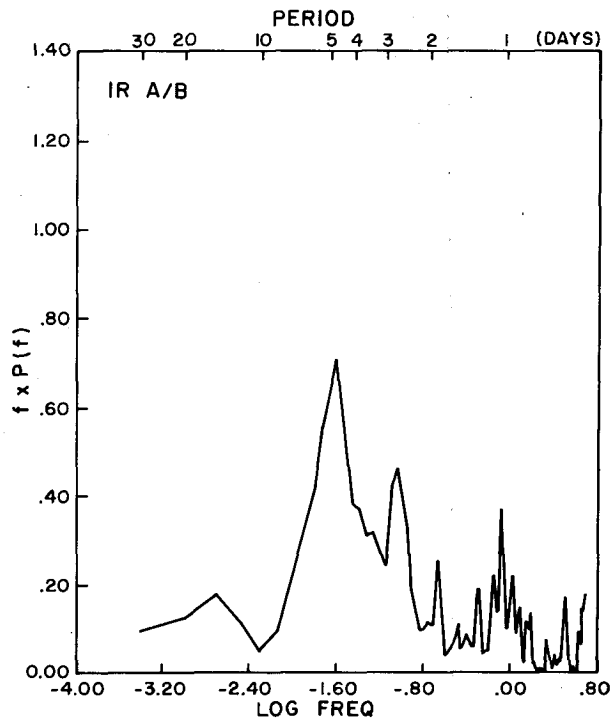

FIG. 6. Power spectrum of IR variation averaged over the A/B area.

analysis to the upper air observation data processed over the A/B area as described in Section 2. Unlike IR data, upper air observation during GATE is intermittent, consisting of three separate phases. The problem is that the length of each GATE phase (~20 days) is not long enough compared with the 4–5 day periodicity. Fortunately this can be overcome by using a recently advanced technique called the Maximum Entropy Method (MEM). Spectral analysis based on MEM has the advantage that it gives substantially finer resolution for short record length than the conventional method. The computer program of MEM was given by Hayashi (1977) in the generalized form applicable to complex variables. He also demonstrated its advantages in the same article.

Fig. 7 shows an example of the resultant spectra. It is obtained from the time series of the large-scale vertical p-velocity over the A/B area during Phase III (30 August–19 September) of GATE. During this period the line of maximum cloudiness is usually located well within the A/B area (Sadler, 1975), giving us a typical situation to investigate the vertical motion. The manner of presentation in this figure is the same as in Fig. 6 except that the values are plotted as a function of height and log frequency. One can see that vertically persistent peaks appear around a 4–5 day period and near a diurnal period. The former shows large power in the lower troposphere between 700 and 500 mb and in the upper levels around 300 mb; the latter shows the maximum to be around the 600 mb level. The large power near the Nyquist frequency (0.5 day in period) turned out to be artificial due to the existence of a white noise component (see Zangvil, 1977). Although figures are not shown in this paper, the 4–5 day peak and the diurnal peak have also been obtained in the time series of other quantities such as vorticity and temperature.

Comparing these results with the ones in Fig. 6 obtained from IR data, we can see that the 4–5 day and diurnal peaks agree well with each other. However, the peak around a 2.5-day period in IR does not have its counterpart in the vertical p velocity. In fact, Fig. 7 shows minimum power around a 2-day period. This lack of evidence in such an important variable as vertical motion makes the interpretation of the 2-day mode somewhat puzzling. At present we anticipate this to two possibilities. One is that the 2-day peak in IR may be a false one which has no physical substantiality. Another is that this mode may be associated with a mesoscale or medium-scale structure in the atmosphere as discussed by Murakami (1972) and Orlanski and Polinsky (1977), so that it can be detected only when we use a much smaller area than the present one. In fact, Murakami (1972) demonstrated that such was the case for short-period disturbances over the Marshall Islands area.

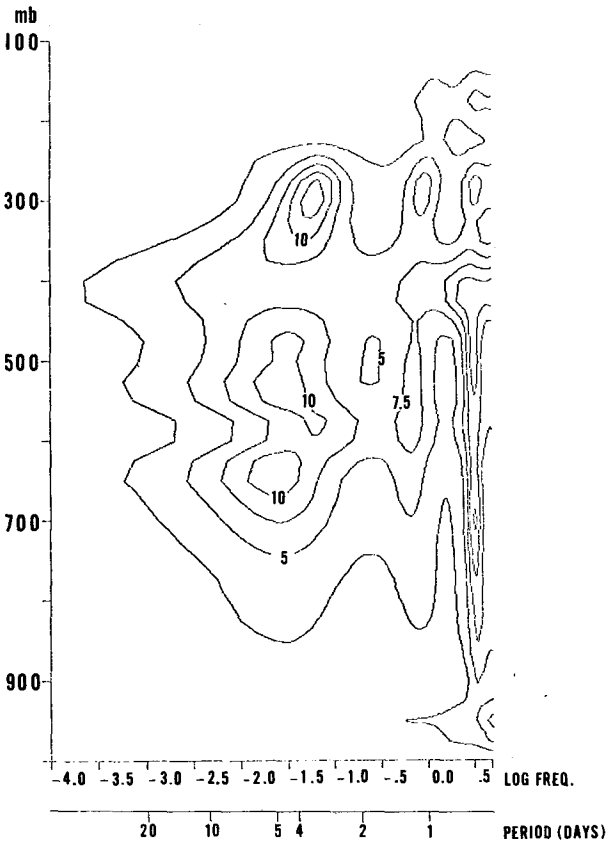

FIG. 7. Vertical distribution of power spectra of the spectra of vertical p velocity during Phase III of GATE. Units are $mb^2\ h^{-2}\ day^{-1}$.

Though the latter seems more likely, these two possibilities remain to be examined in further investigation.

In any case, results indicate that the 2-day IR mode is poorly correlated with the large-scale field of the atmosphere. For the moment, therefore, we put aside the investigation of this mode and concentrate our concern on the 4–5 day period and the diurnal mode which show good association with the large-scale field. In the following sections, we shall discuss their horizontal character over the eastern Atlantic in terms of IR and also discuss the structure of the associated disturbances over the A/B area.

4. Characteristic behavior of transient modes

a. The 4–5 day mode

In this section we shall discuss the space-time behavior of the two transient modes, namely, the 4–5 day and diurnal modes. We first investigate the 4–5 day mode. In order to do so, we should separate this particular mode from the other variations of different time scale which are superposed

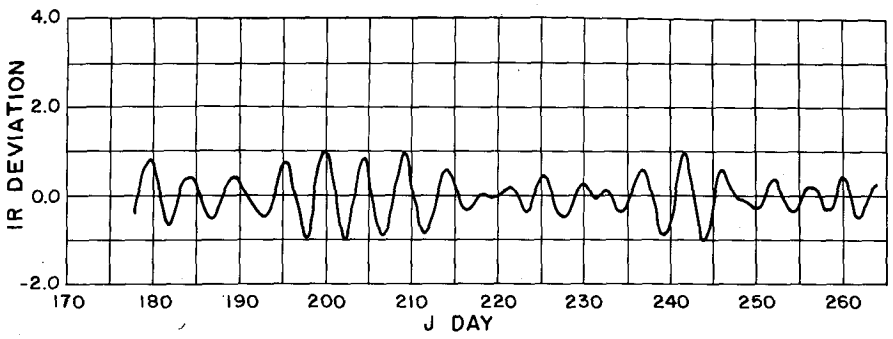

FIG. 8. As in Fig. 4 except for the bandpass filtered time sequence.

in the original time series. This task was carried out by applying a bandpass filter based on the so-called recursion technique. This technique gives us far more rapid convergence than the conventional filter based on weighted averages. In addition, it has the advantage that we can specify the peak in the response curve, and its bandwidth, arbitrarily. The principle of this technique and the response function used in this study are described in the Appendix.

Fig. 8 represents the bandpass filtered time sequence of IR counts averaged over the A/B area. Its original time sequence can be seen in Fig. 4. Comparing both figures, one can see that the peaks in Fig. 8 agree well with the major enhancements (positive anomalies) appearing in Fig. 4. This fact verifies that the present bandpass filter has picked up the right phase angle of the temporal variation. At the same time it indicates that the 4–5 day mode is making a major contribution to the large-scale enhancement of convective activity over the A/B area. Fig. 8 also shows that the amplitude of the 4–5 day mode changes from time to time. For example, the amplitude is large from Day 195 (14 July) through Day 210 (29 July), while it becomes small from Day 215 (3 August) through Day 235 (23 August).

The longitudinal propagation of the 4–5 day mode was examined by using the longitude-time diagram. Fig. 9 exhibits part of the results which cover the same period of a similar diagram previously shown in Fig. 5. It is apparent that the 4–5 day mode in this figure reveals the tendency of westward propagation as discussed by Payne and McGarry (1977) using SMS 1 IR photographic images. While they demonstrated a westward propagation of the convective activity over West Africa and its vicinity, Fig. 9 reveals that it can be well tracked from west Africa through the Atlantic. Furthermore, by comparing this diagram with Fig. 5, we can see that most of the traveling component in Fig. 5 can be accounted for by the westward moving 4–5 day mode. The mean phase speed of this mode over the whole GATE period turned out to be about 7° day^{-1} and the mean longitudinal interval between the enhanced areas is about 30°. These figures are in good agreement with the previous estimates made on the so-called African waves, synoptically by Carlson (1969a,b) and statistically by Burpee (1972, 1974), Reed *et al.* (1977) and others.

b. Diurnal mode

At first, the diurnal variation of the convective activity was examined over the A/B area by using time series of the areally averaged IR counts which was high-pass filtered so that fluctuation with periods longer than 2 days was eliminated. The time composite was then carried out for each observation time. Fig. 10 presents the composited variation in terms of anomalies from the time-mean value. Time in the original data set (GMT) has been transformed into local time by applying a 1.5 h time difference based on the location of the A/B area.

The composited anomalies in Fig. 10 show an apparent diurnal cycle over the A/B area. The maximum appears in the early evening around 1800 LT, while the minimum occurs in the morning around 1000 LT. It was also found that the amplitude of the diurnal cycle was nearly doubled when the composite (not shown) was made on the disturbed period in the sense of a 4–5 day mode (see Fig. 8), but its phase (evening maximum and morning minimum) was kept nearly intact.

The occurrence of a maximum (minimum) in the afternoon (morning) in IR counts is consistent with the previous results obtained from the upper cloudiness (Gruber, 1976; McGarry and Reed, 1978), precipitation (Gray and Jacobson, 1977; McGarry and Reed, 1978) and radar echoes (Marks, 1975) over the A/B area. However, the time at which the maximum activity takes place differs from one result to another. For example, Gruber (1976) reported that maximum upper cloudiness occurred around 1630 LT, while McGarry and Reed (1978) obtained the maximum convective cloudiness around 1400 LT and the present study showed maximum digital IR count around 1800 LT. Considering that different

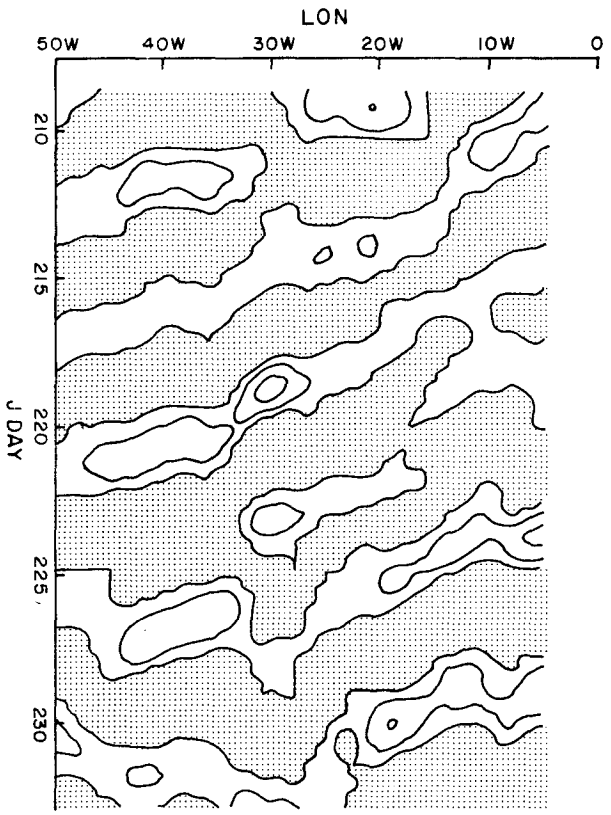

FIG. 9. As in Fig. 5 except for bandpass filtered anomalies. Contours are drawn at every 0.5 intervals for positive anomalies.

quantities have been examined in these studies, the discrepancies may have something to do with the life cycle of convective systems. However, it also seems fair to say that it could be just statistical fluctuation due to the limited amount of data or to different methods of data processing.

Despite the early report by Marks (1975) who examined radar echoes, no obvious indication of a semi-diurnal oscillation has been found in the present study of IR data. On the other hand, Gruber (1976) indicated that the variation of total cloudiness showed a semi-diurnal cycle. Since the digital IR count is apt to reflect the variation of high-top clouds better than low clouds, it seems to indicate that the semi-diurnal mode tends to manifest itself in terms of shallow convection.

So far the occurrence of the maximum convective activity in the afternoon over the A/B area has been taken to be somewhat anomalous by many investigators, because it has been widely believed that oceanic areas shows a maximum in the early morning. Gray and Jacobson (1977) reviewed the evidence for the morning maximum over the ocean and they attributed the afternoon maximum over the A/B area to the influence of squall lines propagating from west Africa. McGarry and Reed (1978) suggested a controlling effect by the wind field, pointing out that the subregional fluctuations in the phase and the amplitude of the diurnal mode over the eastern Atlantic is not likely to be due to pure radiative control. In any case, it seems worthwhile for us to look into the spatial aspects of the diurnal mode over the ocean.

Satellite-observed IR data have a special advantage for this purpose in the sense that they can provide us with a large amount of data over the ocean where other observations are sparse. In the present study, time series of the IR counts at each 1° by 1° mesh were high-pass filtered by the same filter as was used in obtaining Fig. 10 and then composited at each observation time. Fig. 11a–11d show the horizontal distributions of the composited diurnal anomalies at 0000, 0600, 1200 and 1800 GMT, respectively. Contours are drawn at every 0.2 counts and negative anomalies are shaded. Since the composition was made with respect to GMT, the corresponding local time was plotted on each map along with the longitude.

Over the ocean, the shaded (negative) areas reflect the suppression of high-top clouds, indicating low convective activity over the same area. Over land, however, we should be cautious because it turned out that the IR variation over this area was contaminated by the intense diurnal cycle of the ground temperature. For instance, we can see large positive anomalies over West Africa and South America in Fig. 11a which represents the situation near midnight, but these positive anomalies may be interpreted as a manifestation of cold ground temperature at night rather than the high convective activity. For this reason, we shall restrict our discussion to the oceanic area for the moment.

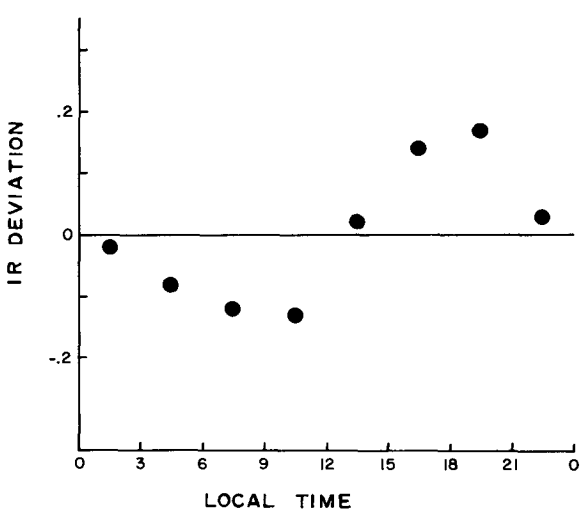

FIG. 10. Composited diurnal variation of IR data averaged over the A/B area.

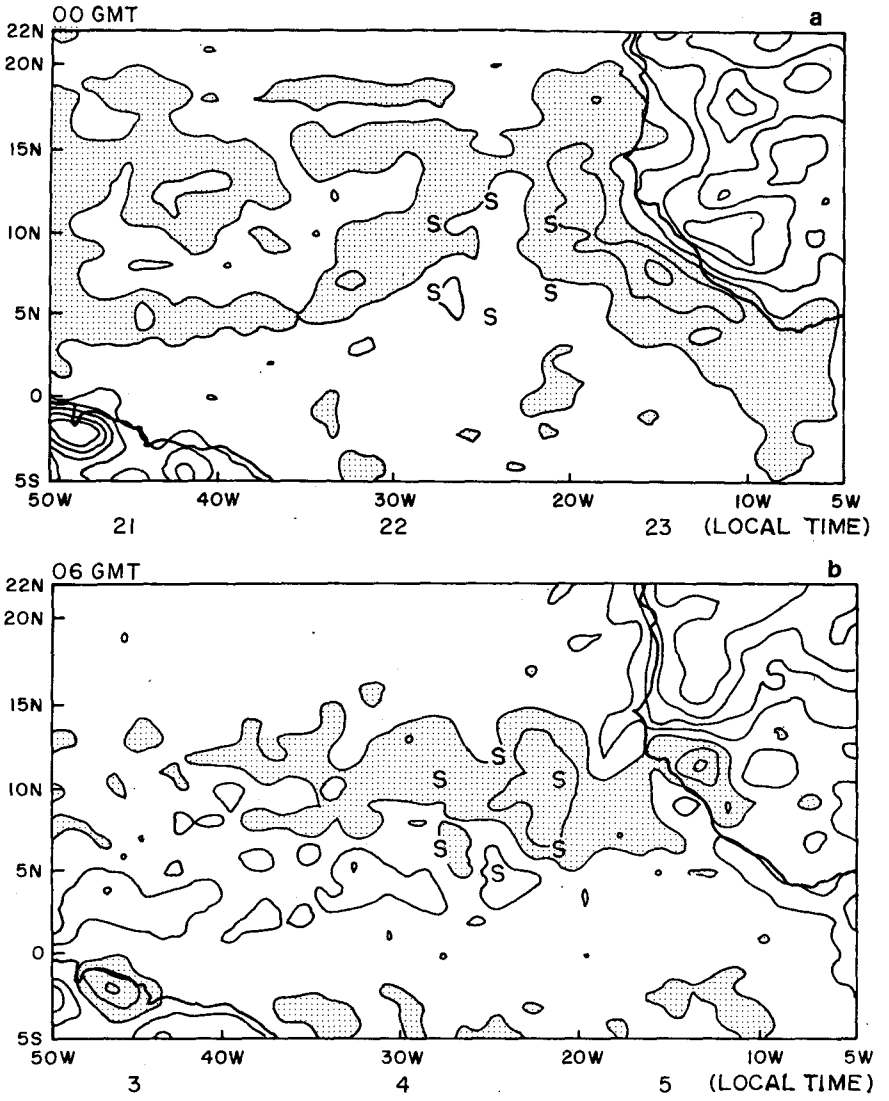

FIG. 11. Horizontal distribution of composited diurnal anomalies of IR data at (a) 0000, (b) 0006, (c) 1200 and (d) 1800 GMT. Contour interval is 0.2 units. S's as in Fig. 3. Local time indicated along abscissa.

Fig. 11a shows the distribution of diurnal anomalies at 0000 GMT, i.e., near midnight over the eastern Atlantic. Despite the relative uniformity of the nocturnal radiative effect, we can see an apparent inhomogeneity in the distribution over the Atlantic. An intensively suppressed area appears along the coast of West Africa at this time. Its configuration seems to suggest the influence of the African continent on the deep convective activity over the surrounding ocean. If this is the case, the offshore width of the suppressed area (roughly 500 km) also indicates the extent to which the African continent exerts its influence. Over the middle Atlantic the configuration appears somewhat irregular, probably just showing the transition phase from the overall suppression to enhancement as will be discussed subsequently.

The distribution in the early morning is exhibited in Fig. 11b. By this time, the suppressed condition along the coast of West Africa vanishes. Instead, one can see the zonally oriented configuration of the suppressed area which runs just through the main portion of the A/B area. This is consistent with the appearance of negative anomalies in Fig. 10 which shows the areally averaged values over the A/B area. It is interesting to note that the positive anomalies of comparable magnitude take place in Fig. 11b to the south of the negative area at the same time. This means that we could have observed the maximum

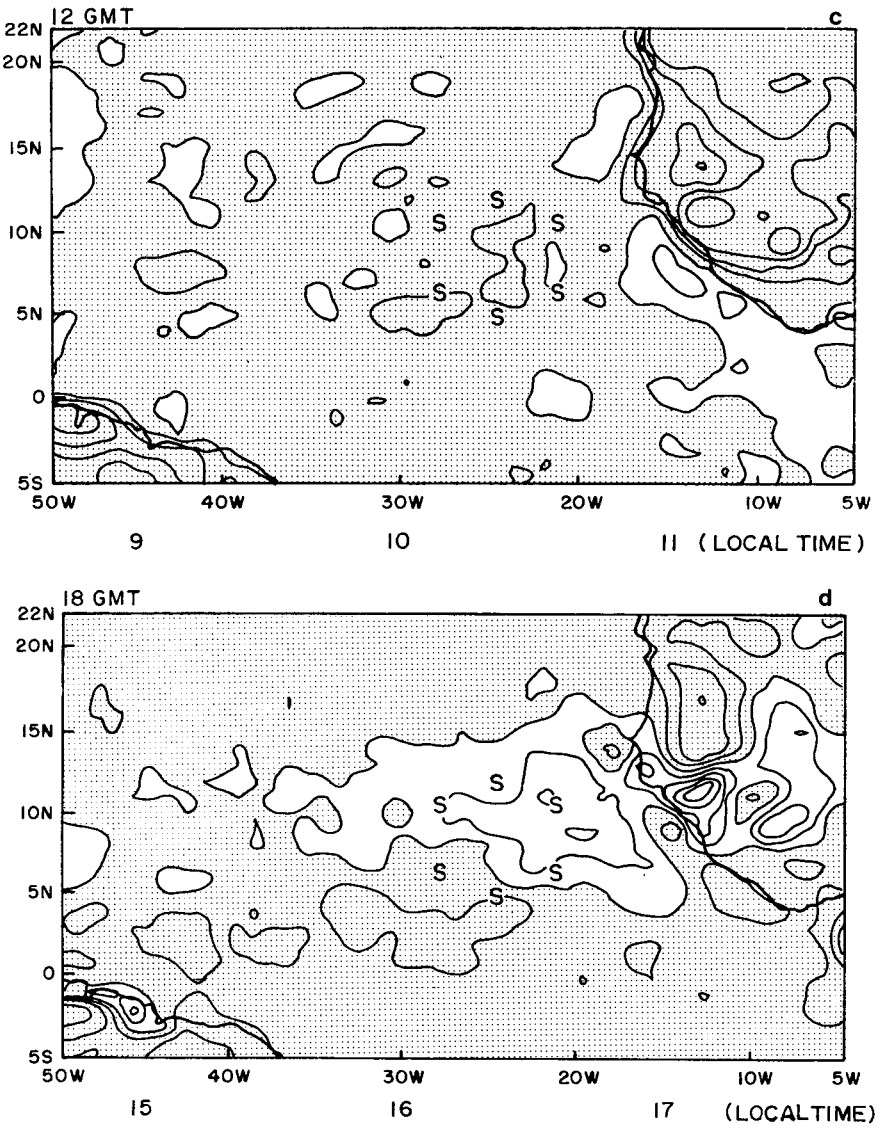

FIG. 11. (*Continued*)

convective activity in the early morning if the A/B area had been located further to the south. When we compare this configuration with the distribution of mean IR counts shown in Fig. 3, it appears that the early morning maximum tends to occur to the south of the axis of maximum mean values. Likewise, the morning minimum tends to appear to the north of the same axis over the Atlantic.

Fig. 11c shows the distribution near local noon. At this time, the overall situation for the eastern Atlantic indicates suppressed convective activity except for the vicinity of West Africa. Along the coast of this continent, the maximum enhancement occurs in the early afternoon around 1400 LT (not shown). This behavior near the coast agrees with the results shown by McGarry and Reed (1978) in Fig. 2 of their paper in terms of the percent coverage by convective clouds.

As time proceeds, the enhanced area moves westward off the coast of Africa and forms a zonally oriented configuration in the late afternoon over the eastern Atlantic. This situation is exhibited in Fig. 11d. Again one can see that the comparable negative anomalies occur to the south of the enhanced area which runs through the major portion of the A/B area. The situation is nearly the opposite of that in the early morning shown in Fig. 11b. Although we confine our concern to the oceanic area as mentioned before, the intense positive anomalies which appear over the West Africa in Fig. 11d seem remarkable.

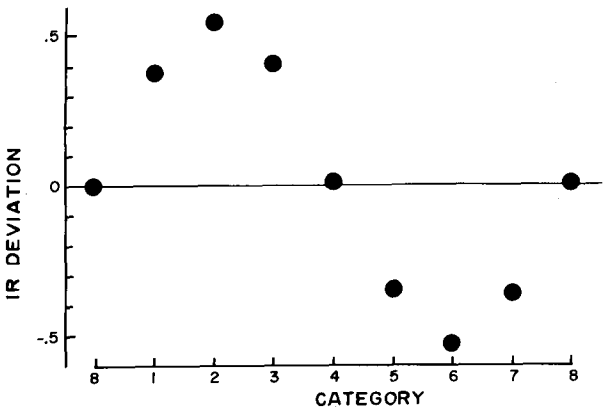

FIG. 12. Composited anomalies of IR data over the A/B area for each category of 4–5 day mode.

These positive values mean cold temperature anomalies despite the relatively warm ground temperature at this time of the day, thus indicating strong enhancement of the convective activity over the same area.

5. Associated disturbances

a. The 4–5 day mode

In the previous section we discussed the large-scale aspects of the convective activity measured by the digital IR data. Our next concern is the kind of disturbances which are associated with the large-scale kinematic and thermal fields. The correspondence of the convective activity to the passage of African waves has been intensively discussed by Payne and McGarry (1977), Reed *et al.* (1977) and Burpee (1975) in their framework of wave composition. Their procedure consists of categorizing the variation of the meridional wind and obtaining the mean structure for each category along the path of disturbances. In this study we shall rather start with categorizing the variation of convective activity and obtain the structure of the disturbances at the very moment when they pass through the GATE A/B area. Accordingly, we did not include any coastal or inland observations when making a composite, because we cannot yet exclude the possibility that the structure of the disturbance differs over land and the ocean areas.

In order to make a composite of the 4–5 day mode, the bandpass filtered variation of IR data as shown in Fig. 8 was classified into eight categories. Categories 2 and 6 were assigned to the time when the maximum and minimum anomalies take place, respectively. Category 4 represents the transition from positive anomalies to negative ones and category 8 shows the transition from negative to positive. Categories 1, 3, 5 and 7 were assigned to the intermediate times. Fig. 12 represents the composited anomalies of the averaged IR counts for each category of the 4–5 day mode over the A/B area. Since one cycle of this mode was divided into eight, the interval between the categories is equivalent to the time interval of 0.5–0.6 day (or ~12 to 14 h).

The same categories were applied to the bandpass filtered variations of the large-scale quantities over the A/B area. These quantities consist of large-scale vertical and horizontal motion, temperature and moisture. They are obtained from the upper air observations of GATE ships located within the same area and processed following the procedure described in Section 2. The problem that each phase of GATE is not long enough for the conventional, weighted-average-type filter was overcome by employing a recursion technique which is explained in the Appendix.

Fig. 13 represents the vertical cross section of the composited anomalies of the vertical p velocity. The stippled area indicates negative anomalies which mean upward motion. At category 2 which presumably corresponds to the most enhanced convective activity, the upward anomalies take place in the large-scale vertical motion throughout the troposphere. This is quite consistent with what has often been reported as evidence of the large-scale control on convective activity, though one would notice the existence of a time lag in this figure between the maximum convective activity and the intensified large-scale upward motion. It appears that a low-level maximum of the upward motion, which indicates the concentrated convergence below, precedes the maximum convective activity, while the profile at category 2 shows one major maximum at upper levels around 400 mb indicating the deep convergence layer below. A similar sequence except for the opposite sign holds at category 6, which represents the suppressed period of convective activity.

Fig. 14 shows the composited anomalies of the meridional wind in which the stippled area represents north wind anomalies. At category 2 one can see that the south wind anomalies take place in the lower troposphere while the relatively intense north wind anomalies appear in the upper levels. We can also see the apparent phase lag with height in the meridional wind variation except for the uppermost and lowermost layers. These configurations give us further implications when we take into account the spatial aspects of the 4–5 day mode revealed in Section 4a. As discussed in that section, the disturbances of this mode propagate westward through the GATE A/B area. Considering this fact along with the above configuration, it emerges that the maximum convective activity at category 2 is located to the east of the low-level trough in concur-

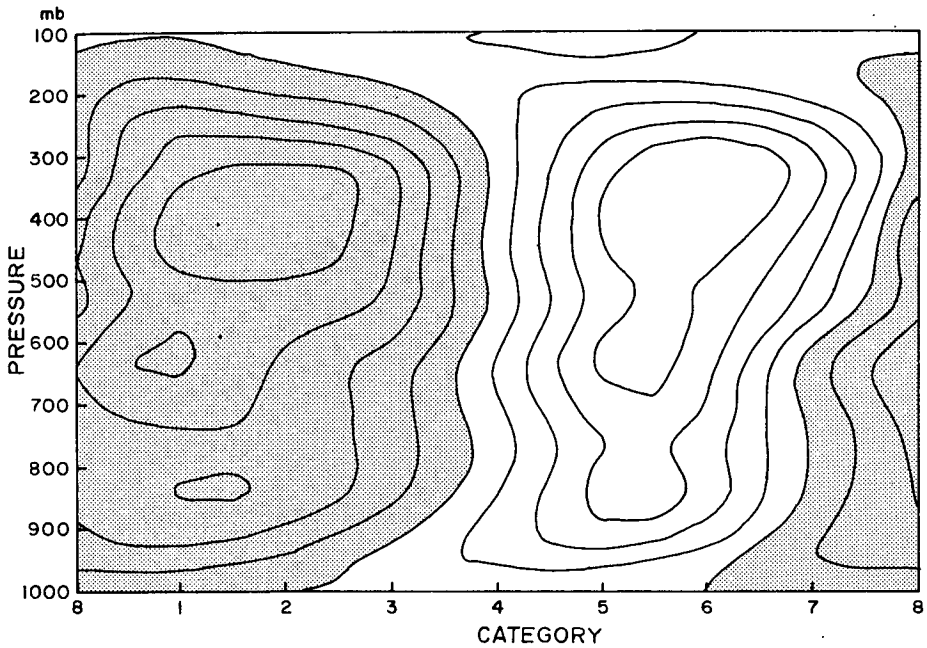

FIG. 13. Vertical cross section of composited anomalies for the vertical p-velocity over the A/B area. Contours are drawn at 0.2 mb h^{-1} and negative values are shaded.

rence with the south wind anomalies. In Fig. 14, the trough axis can be specified as the transition line through which north wind (negative) anomalies turn into south wind (positive) anomalies. Therefore, the phase lag with height which was mentioned above means that the axis of the trough tilts eastward with height over the A/B area.

This structure differs somewhat from the one obtained by Reed *et al.* (1977), although the location of the maximum convective activity in the present

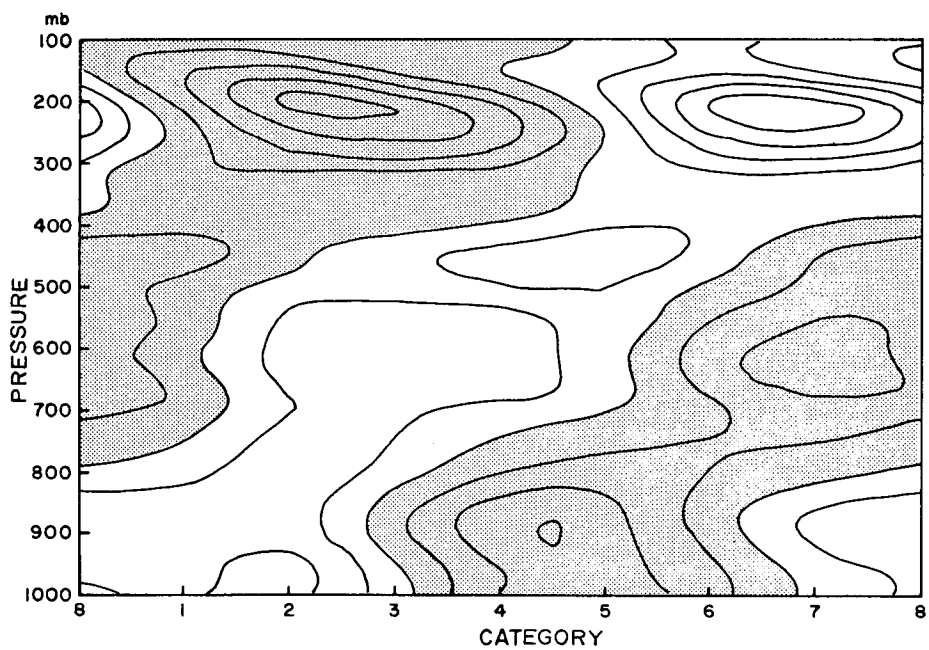

FIG. 14. As in Fig. 13 except for the meridional wind component. Contours are drawn at every 0.25 m s^{-1}.

study agrees with Burpee's (1975) composite where it was found that the intensified upward motion and the northward-advanced upper level clouds take place east of the 700 mb trough. Recently, Thompson *et al.* (1979) and Nitta (1978) applied a similar procedure to the upper air observations over the same A/B area used in this study. Their composite showed that the enhanced convective activity and the upward motion tend to occur just above the trough rather than to the west of it, again differing somewhat from the results in this study. Presently, we speculate that three possibilities could account for the contrast.

First, their composites were based on the data obtained during Phase III (30 August–19 September, 1974) of GATE, while the present one has been made by utilizing all three phases. This could cause the difference in the resultant structure, because it seems that the mean latitude through which the disturbances travel changes from one phase to another. It is likely that the disturbance shows different vertical structure at different latitudinal distances from the center. Although we discuss only the time-mean structure in this paper, the foregoing aspect deserves consideration and should be the subject of further investigation.

Second, we have used bandpass filtered data when making our composite instead of the raw data used by the other investigators. Using bandpass filtered data has an unfavorable impact because it almost invariably reduces the amplitude of the composited disturbances by smoothing the sharp peaks in the original time series. However, under conditions where variations due to the different time scales coexist and possibly interact with each other, use of the raw data could cause a certain amount of contamination in the result.

The third possibility is that we started with categorizing the variation of convective activity rather than with the meridional wind as was done in the other studies. Although starting with the convective activity is more reasonable in the sense that we can look directly into the associated variation in the large-scale atmospheric fields, the relatively unfixed behavior of the convective systems in the framework of large-scale disturbances may have caused some blurring effects in the resultant composites.

Regarding the location of the maximum convective activity, it is also of some interst to note that Carlson (1969a) has reported evidence of a secondary maximum in the disturbed conditions located to the east of the trough when it propagates over Africa. The present result over the A/B area might imply that this secondary maximum turns into the major one when the disturbance reaches the Atlantic Ocean.

Fig. 15 shows the composited anomalies in the temperature variation associated with the 4–5 day mode. At category 2, cold anomalies appear in the lower troposphere below the 600 mb level, while warm anomalies take place above that level. However, one can see that the relatively intense cold anomalies appear again in the uppermost layer between the 200 and 100 mb levels. These cold anomalies may be an indication of the effect due to cirrus canopies above the deep convective clouds, but it is also possible that they come from the overshooting effect of convective clouds or from temperature advection associated with the wave disturbance.

Comparing this diagram with Fig. 14, one can see that the cold anomalies coincide with the south wind anomalies when they show an eastward tilt with height, while the cold and the north wind anomalies appear concurrently when their axes tilt westward with height. This configuration proves physically consistent when we take into account the hydrostatic and quasi-geostrophic balance which presumably holds for the wave disturbance of this scale.

Fig. 16 exhibits the composited anomalies of mixing ratio in which positive (moist) anomalies are stippled. At the stage of the most enhanced convective activity represented by category 2, moist anomalies are carried through the lower to the upper troposphere which presumably corresponds to the cloud layer in the tropical atmosphere. However, it is interesting to see that the lowermost layer of the troposphere below the 900 mb level shows dry anomalies at this stage. This layer roughly corresponds to the vertical extent of the subcloud layer and the decrease in mixing ratio seems to indicate the effect of cloud-induced downward motion as discussed by Betts (1976). The occurrence of a similar situation has been also reported by Frank (1978) when cloud clusters or squall lines pass over the GATE A/B area.

b. Diurnal mode

The time-composite technique was also applied to the upper air observation over the A/B area for the purpose of investigating the diurnal variation in large-scale quantities. The original data set was the same as used in the previous subsection, but at this time a high-pass filter was applied before making a composite in order to suppress the oscillations with periods longer than 2 days. Since the present data set was arranged in such a way that it yields observations at 6 h intervals during the three phases of GATE, the composition was carried out with respect to local time. This relatively coarse resolution compared with that of IR data (3 h) limited our analyses of the diurnal mode. Therefore, no effort has been made in this study to construct

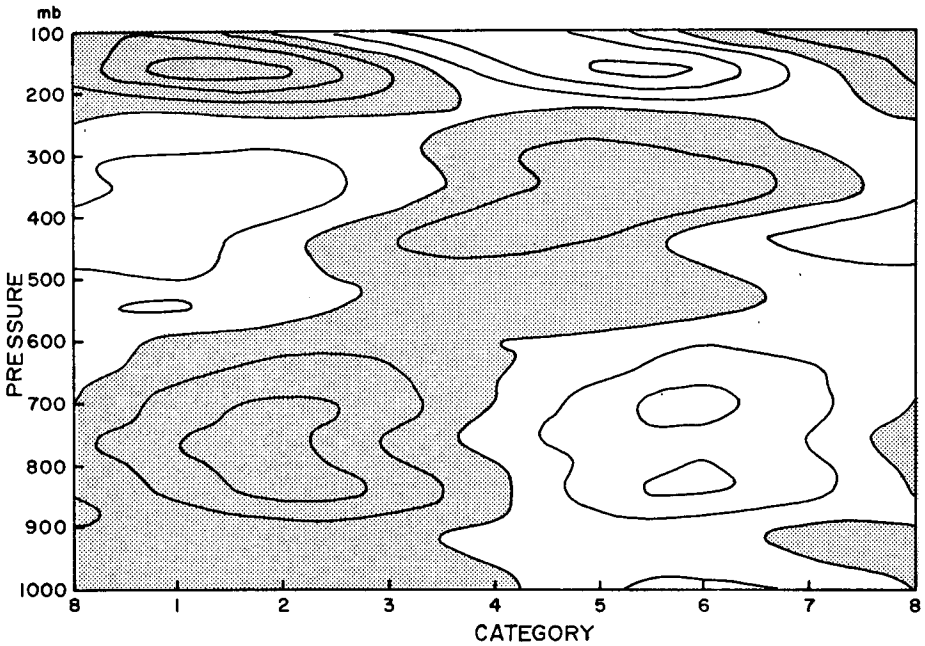

FIG. 15. As in Fig. 13 except for temperature. Contours are drawn at every 0.1 K.

a smooth, time-varying diagram as illustrated in the previous subsection, nor to discern the difference between the so-called "disturbed" and "suppressed" situations.

Fig. 17 shows the vertical distributions of composited diurnal anomalies in the vertical p-velocity, temperature and the mixing ratio at four local times. They represent the mean diurnal variation during the three phases of GATE over the A/B area. What appears most apparent in these profiles is the behavior of the vertical p-velocity which shows positive (downward) anomalies during the night and negative (upward) anomalies during the daytime. The most intense downward anomalies occur near

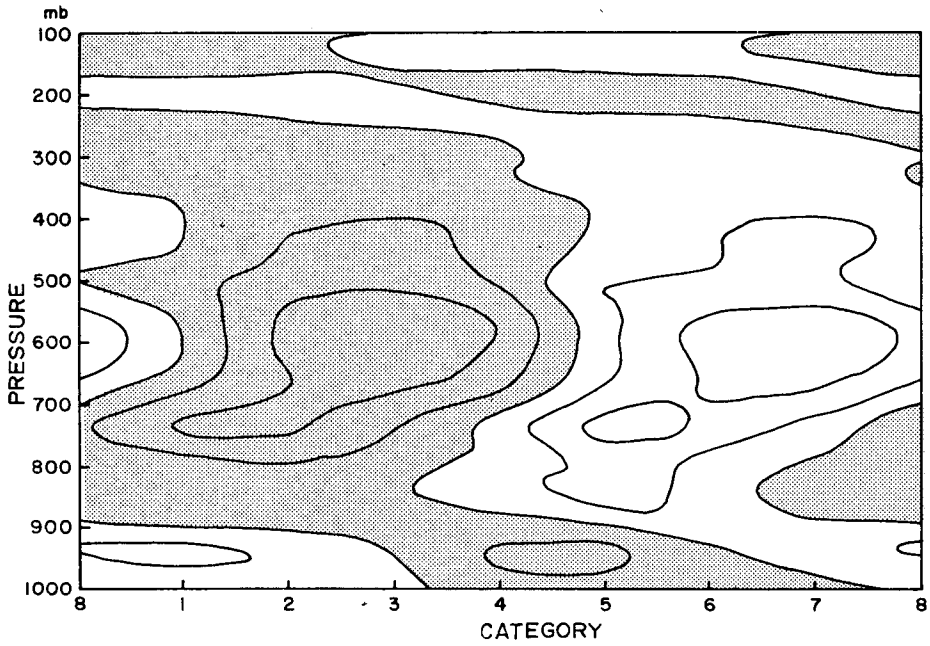

FIG. 16. As in Fig. 13 except for the mixing ratio. Contours are drawn at every 0.1 g kg^{-1}.

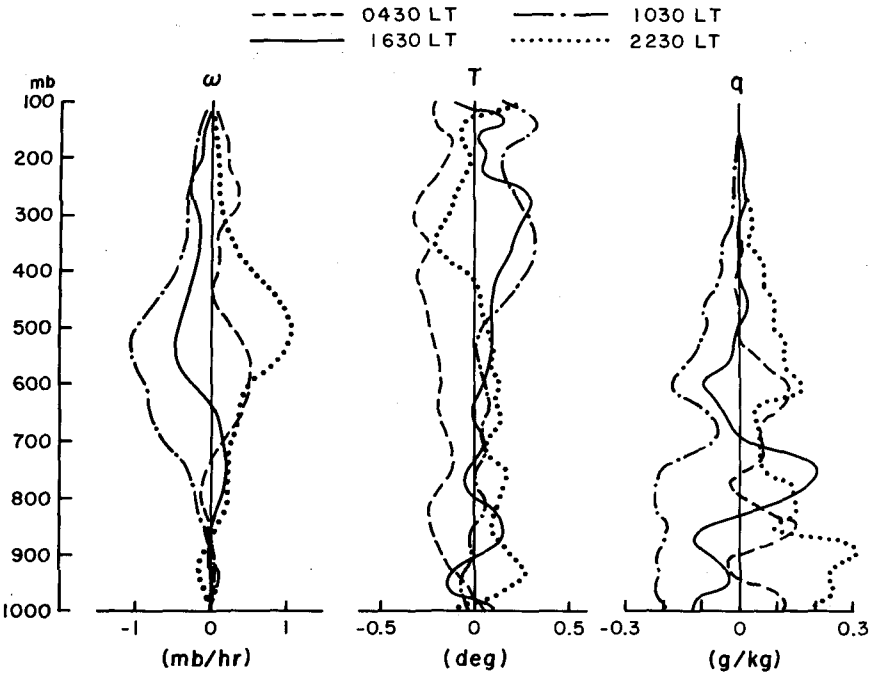

FIG. 17. Vertical distribution of the composited diurnal anomalies in the vertical p velocity (left), temperature (middle) and mixing ratio (right).

midnight (2230 LT), while the intense upward anomalies take place near local noon (1030 LT). Profiles at both times show major peaks around the 500 mb level, indicating the existence of a deep divergent (convergent) layer below at night (day).

Though we cannot depict the detailed time sequence by the present 6 h composite, the above tendency agrees quite well with the one obtained by Dewart (1977) who intensively investigated the diurnal variation in the large-scale quantities over the A/B area. In her composited time-height diagram of diurnal anomalies, it was shown that upward anomalies reach their maximum at 1330 LT and the maximum downward anomalies appear at 2230 LT when averaged over the GATE period. Recently Pedder (1978) also obtained similar phases for the diurnal component in the vertical p velocity over the same area.

Temperature deviations in the middle of Fig. 17 show that the amplitude of the diurnal variation is larger in the upper troposphere than that at lower levels. In the upper troposphere, it can be seen that warm anomalies occur during the day, while cold anomalies take place at night. Its amplitude appears to be about 0.3 K in the present high-pass filtered data. In the lower troposphere the situation seems slightly different and the amplitude is smaller. In these levels cold anomalies occur consistently in the early morning (0430 LT), but the late evening (2230 LT) shows warm anomalies in contrast with the upper levels. It also seems that the daytime warming near the surface is not dominant over this oceanic area, quite different from the situation over the land.

The deviations of mixing ratio are shown in the right part of Fig. 17. As one would readily anticipate, the amplitude of the diurnal variation is large in the lowermost troposphere and tends to decrease upward. It also appears characteristic that the atmosphere shows overall dryness in the late morning near local noon (1030 LT) and moist anomalies occur throughout the troposphere in the late evening near midnight (2230 LT). Deviations at 0430 and 1630 LT fluctuate near zero, probably just reflecting the transitional phase from positive to negative and its reverse, respectively. Dewart (1977) discussed the similar tendency in terms of precipitable water. She showed that the precipitable water becomes minimum in the vertical column between the 900 and 500 mb levels at 1030 LT and becomes maximum at 1930 LT.

In comparing these results with the composited variation of IR shown in Fig. 10, it emerges that the enhanced IR counts in the late afternoon are associated with the warm anomalies in the upper troposphere. However, the variations in vertical motion and mixing ratio at this time show transitional aspects rather than extremes. Considering that the time series of the above quantities have undergone the same processing, it is likely that these

different aspects in different quantities are related to the life cycle of convective systems. For example, it can be seen that the maximum upward motion precedes the maximum IR count over the A/B area. This time difference may be attributed to the fact that the maximum IR count is apt to occur at the mature stage of the convective system in which clouds reach their highest tops and often bear large cirrus canopies. On the other hand, the maximum upward motion is likely to correspond with the developing stage which precedes the mature one.

The behavior of mixing ratio appears somewhat puzzling because it shows dry anomalies at the time when the upward motion becomes intense and moist anomalies when the downward anomalies become large. In order to examine its statistical stability, the same composition was made for each separate phase of GATE. Although the figures are not shown here, it turned out that each phase showed a similar tendency as a mean behavior. This seems to suggest that in the sense of mean diurnal variation, other effects such as horizontal advection may exert more influence than the large-scale vertical advection of atmospheric moisture. However, we should also be aware of the fact that the radiosonde thermistor and hygrister have often shown an artificial diurnal drift due to solar radiation effects. Thorough instrumental calibration is essential before any final conclusions on temperature and humidity can be made.

6. Summary and remarks

In this study we have measured the large-scale convective activity by using the digital IR data averaged over each 1° by 1° mesh in GATE area. The distribution of their time-mean values shows a zonally oriented area of high convective activity which lies between 5 and 10°N over the Atlantic and a little further northward over west Africa. Longitudinally, it is most intense over the coast of West Africa and tends to decrease toward the middle Atlantic. A longitude-time diagram has revealed the existence of vigorous transient disturbances which travel westward from West Africa through the eastern Atlantic. Their activity as measured by anomalous IR counts also tends to be intense near the coast of West Africa and decreases toward the middle Atlantic. However, it was also noted that on some occasions there is a redevelopment of the disturbance in the middle of the Atlantic.

The statistical characters of the temporal variation were examined by spectral analysis. When applied to the time series of IR data averaged over the GATE A/B area, the resultant spectrum shows three remarkable peaks, a 4–5 day period, a 2.5-day period and a diurnal period. Spectra of other large-scale quantities such as averaged vertical motion over the same area also yield notable peaks around a 4–5 day period and the diurnal period, but no obvious 2.5-day period. It is speculated that the 2.5-day mode in convective activity may be associated with meso-scale or medium-scale systems in the atmosphere as suggested by Murakami (1972) and Orlanski and Polinsky (1977). This mode has been temporarily put aside in the present investigation where the objective is to look into the large-scale association between the convective activity and atmospheric systems.

The behavior of the 4–5 day mode in convective activity was investigated using data processed by the corresponding bandpass filter. The longitude-time diagram clearly revealed that the enhanced convective activity associated with this mode propagates westward from west Africa through the eastern Atlantic at a phase speed of about 7° day^{-1} in longitude. Furthermore, the diagram also showed the characteristic longitudinal scale which can be measured by the distance between the adjacent enhanced areas. When averaged over the whole period of GATE, this longitudinal scale turned out to be about 30°.

Comparison between the original and the bandpass filtered diagram showed that the major amount of the transient component in IR variation can be accounted for by this westward moving 4–5 day mode. Considering the abovementioned characteristic features, it has been concluded that this mode corresponds to the so-called African waves which were investigated earlier by Carlson (1969a,b), Burpee (1972, 1974), Reed *et al.* (1977) and others.

The large-scale behavior of the diurnal mode was investigated by the time-composite technique after the original time series was processed by a high-pass filter. The composited IR variation over the A/B area revealed that the convective activity over this area reaches a maximum in the early evening and a minimum in the morning. This result appears to conflict with the frequently reported situation that oceanic areas show maximum convective activity in the early morning and led us to look further into the situation over the Atlantic.

The above task was carried out by making composites for each 1° by 1° mesh over the Atlantic and examining their horizontal distribution at each reference time. It has been revealed that the afternoon maximum of convective activity takes place not only in the vicinity of the African continent, but it also extends further west toward the middle Atlantic. The area in which the afternoon maximum occurs is oriented zonally roughly along 10°N. What is more interesting in the present result is the finding that there is a coexistence of another area which shows an early morning maximum. Moreover, the former

area seems to be located just to the south of the latter. This situation is especially obvious to the west of 20°W over the tropical Atlantic.

Comparing the above configuration with the mean axis of the maximum IR counts during the same season, it appears that the afternoon maximum tends to occur to the north of it, while the morning maximum takes place to the south. This situation has raised the speculation that the parallel of latitude along which convection is enhanced may oscillate diurnally, i.e., advances northward during the day and retreats southward at night. It is likely that the above aspect has something to do with the diurnal oscillation in the intensity of the low-level easterly jet over the same region. In any case, however, further investigation is definitely needed before we draw any conclusion.

The atmospheric system associated with each mode of the convective activity was then investigated by using upper air observation data over the GATE A/B area. The bandpass filtered variation of IR data was first classified into eight categories in order to investigate the 4–5 day mode. Then, referring to these categories, upper air data were composited to yield a vertical cross section of the associated anomalies. The results showed that the enhanced convective activity is concurrent with the upward anomalies in the large-scale vertical motion throughout the troposphere. In addition, it was also shown that the occurrence of the maximum upward velocity in the lower troposphere precedes the maximum enhancement of convective activity. This indicates that the large-scale convergence in the lower layer tends to occur prior to the enhancement.

The composite of the meridional wind revealed that the maximum enhancement of the convective activity is concurrent with south wind anomalies in the lower troposphere and north wind anomalies in the upper levels. When we take into account the propagation of the disturbance, this situation means that the maximum convective activity is located to the east of the trough in the lower troposphere and there is an anticyclonic circulation in the upper troposphere above the low-level trough.

The distribution of temperature anomalies showed that the cold anomalies in the lower troposphere and the warm anomalies in the middle to upper troposphere are associated with the maximum convective activity due to the 4–5 day mode. However, it also showed that the cold anomalies appear again in the uppermost levels near the tropopause at the same stage. The mixing ratio anomalies indicated that the enhanced convective activity is associated with moistening in the cloud layer which extends roughly from 900 to 200 mb, but the drying appears in the subcloud layer below the 900 mb level. This drying in the subcloud layer seems to imply the effect of the cloud-induced downward motion as discussed by Betts (1976).

Through the investigations mentioned above, it has emerged that there are some contrasts between the present structure and the one obtained by Reed *et al.* (1977), especially as to the location of the enhanced convective activity with respect to the low-level trough of the disturbance. The present analysis of the A/B area has shown the maximum enhancement to be to the east of the trough, while their result showed the major enhancement to be to the west of the trough. Though the detailed discussions are not repeated here, several causes have been suggested which could account for the difference.

Diurnal variation in the large-scale atmospheric quantities over the A/B area have also been investigated by making a time composite with respect to the local time. Despite the relatively coarse time resolution (four per day) in the upper air observations, results have revealed that the large-scale vertical motion shows downward anomalies during the night and upward anomalies during the day. The occurrence of the maximum upward motion seems to precede the maximum enhancement of IR count, presumably indicating the different stages in the life cycle of convective systems to which each quantity responds.

Diurnal variation in temperature showed large amplitude in the upper troposphere, where the warm anomalies take place during the day and cold anomalies appear during the night. Unlike the situation over land, the diurnal amplitude of temperature is small in the lowermost troposphere over the A/B area. On the other hand, atmospheric moisture shows large amplitude in the lower levels when measured in terms of the mixing ratio. It appears that the maximum moistening occurs in the late afternoon near midnight while the maximum dryness takes place near local noon. The fact that the occurrence of the maximum dryness coincides with the maximum upward motion seems to suggest that effects other than large-scale vertical advection should be taken into account to explain the diurnal behavior of atmospheric moisture over that area. However, it should also be mentioned that the temperature and the humidity measurement had often suffered an instrumental diurnal drift before GATE was conducted. Although conditions may have been improved by that time, there is still no guarantee that the GATE radiosonde was totally free from that drift. Therefore, it would be fair to regard the above discussion as tentative until a thorough instrumental calibration is carried out.

Nonetheless, the results which have been discussed so far have made it clear that the large-scale variation in the cumulus convective activity can be

characterized by a certain time scale and this variation is associated with a corresponding variation in large-scale atmospheric quantities. However, rigorously speaking, the results of the composite analysis show nothing more than concurrent phenomena in different quantities, they can give good insight as to the large-scale controlling effect on cumulus convective activity. The mechanism in which the large-scale field controls convection still remains to be investigated. It has been anticipated that one would have to employ a cumulus, large-scale interaction model in order to accomplish this purpose.

APPENDIX

Recursion Technique for Band-pass Filter

Digital filtering which has appeared in the past meteorological literature was often carried out by convolving the input time series with the weighting function of the filter. If we have N values of an input series, this procedure can be expressed as

$$y_k = \sum_{i=-M}^{M} w_i x_{k-i}, \tag{1}$$

where $(x_0, x_1, \ldots, x_{N-1})$ are the N values of the input series $(w_{-M}, w_{-M+1}, \ldots, w_M)$ are the $2M + 1$ values of the weighting function and $(y_{-M}, y_{-M+1}, \ldots, y_{N+M-1})$ are the $N + 2M$ values of the output series.

Usually, the portion of the output series which consists of $(y_M, y_{M+1}, \ldots, y_{N-M-1})$ can be regarded as reliable results and $(2M + 1)$ multiplications per one output are required in this portion. Although this computing time is not a serious problem in usual meteorological analysis, the cutoff problem in the output could be crucial when the data length is not long enough compared with the desired periodicity.

Using the so-called Z-transform (Jury, 1964), Eq. (1) becomes

$$Y(Z) = W(Z)X(Z), \tag{2}$$

where

$$X(Z) = \sum_{l=0}^{N-1} x_l z^l, \quad W(Z) = \sum_{l=-M}^{M} w_l z^l,$$

$$Y(Z) = \sum_{l=-M}^{N+M-1} y_l z^l.$$

In this equation, z can be a complex variable and its positive (negative) power represents delay (advance) operation in units of sampling interval. One can easily see that $W(e^{-i\omega\Delta T})$ gives the response function $R(\omega)$ of the digital filter where ΔT represents the sampling interval.

Now, we assume $W(Z)$ can be expressed by the rational function of Z, i.e.,

$$W(Z) = \frac{A(Z)}{B(Z)}, \tag{3}$$

where

$$A(Z) = \sum_{l=0}^{n} a_l z^l,$$

$$B(Z) = \sum_{l=0}^{m} b_l z^l.$$

Substitution of Eq. (3) into (2) yields

$$B(Z)Y(Z) = A(Z)X(Z). \tag{4}$$

By picking up the coefficients of the same power of Z from both sides, we obtain

$$\sum_{l=0}^{m} b_l y_{k-l} = \sum_{l=0}^{n} a_l x_{k-l}. \tag{5}$$

Since we can always put $b_0 = 1$ without loss of generality, Eq. (5) can be expressed as

$$y_k = \sum_{l=0}^{n} a_l x_{k-l} - \sum_{l=1}^{m} b_l y_{k-l}. \tag{6}$$

This equation gives another way to compute the filtered output by using only the present and past input along with the past output. However, it should be noted that the "feedback" mechanism represented by the second term in the right-hand side of (6) can cause instability if the root of $B(Z) = 0$ is located within the unit circle on the complex Z plane.

Shanks (1967) intensively exploited the above technique of recursive filtering. He demonstrated one band-pass filter based on the eighth-order "Butterworth" (Guillemin, 1957) function. However, since the rate of convergence of the higher order filter becomes slower and it turned out that even the lowest order bandpass filter gives us a powerful tool to pick up the desired periodicity rapidly, we constructed another bandpass filter based on the first-order Butterworth function. In our filter the bandpassed output can be obtained by

$$y_k = a(x_k - x_{k-2}) - b_1 y_{k-1} - b_2 y_{k-2}. \tag{7}$$

The corresponding function $W(Z)$ is given by

$$W(Z) = \frac{a(1 - Z^2)}{1 + b_1 z + b_2 z^2}. \tag{8}$$

Note that Eq. (7) requires only two data points in the past. In fact, this filter converges so rapidly that we almost need not worry about the cutoff problem after the procedure which will be mentioned below.

In order to specify the coefficients a, b_1 and b_2, we must determine two out of three frequencies ω_0, ω_1 and ω_2 (measured by 2π/period). ω_0 denotes the one at which we can get a 1.0 response; ω_1 and ω_2 are the ones at which we can get a 0.5 response on both sides of ω_0. Once the two of them are specified, the rest should be the one which

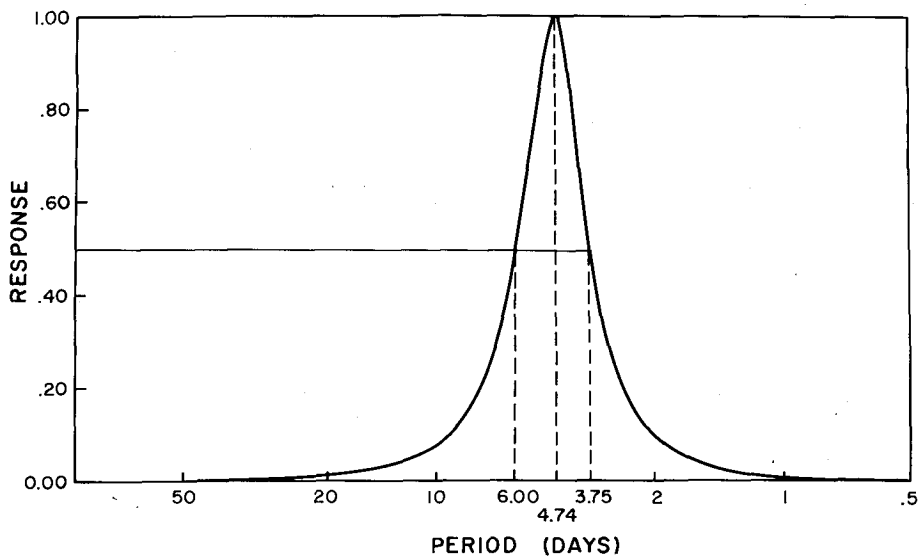

FIG. 18. Response of the bandpass filter used in this study.

satisfies the relation

$$\omega_0^2 = \omega_1\omega_2. \tag{9}$$

Then by knowing the sampling interval ΔT, (a,b_1,b_2) can be specified as

$$a = \frac{2\Delta\Omega}{4 + 2\Delta\Omega + \Omega_0^2},$$

$$b_1 = \frac{2(\Omega_0^2 - 4)}{4 + 2\Delta\Omega + \Omega_0^2},$$

$$b_2 = \frac{4 - 2\Delta\Omega + \Omega_0^2}{4 + 2\Delta\Omega + \Omega_0^2},$$

where

$$\Delta\Omega = 2\left|\frac{\sin\omega_1\Delta T}{1 + \cos\omega_1\Delta T} - \frac{\sin\omega_2\Delta T}{1 + \cos\omega_2\Delta T}\right|,$$

$$\Omega_0^2 = \frac{4\sin\omega_1\Delta T \sin\omega_2\Delta T}{(1 + \cos\omega_1\Delta T)(1 + \cos\omega_2\Delta T)}.$$

The actual calculation consists of two steps in the same manner as Shanks (1967). At the first step, the tentative output is calculated by applying Eq. (7) to the input data from which the mean value and linear trend are removed. Then this output is reversed in time and processed again to obtain the final output. This procedure results in a zero phase shift for all frequencies, while the amplitude response is given by

$$\left|W(e^{-i\omega\Delta T})\right|^2.$$

Fig. 18 shows the response of the bandpass filter used in this study.

Acknowledgment. This study was carried out during the author's stay at Florida State University. The author wishes to express his thanks to Prof. T. N. Krishnamurti for his encouragement and valuable discussions throughout the work. Thanks are also due to Dr. Eric A. Smith of Colorado State University for providing the correction program for IR data. The research reported here was supported by the Atmospheric Sciences Section, National Science Foundation, under Grant ATM75-18945. Part of the calculations were performed on the CDC 6600/7600 system of the National Center for Atmospheric Research. The National Center for Atmospheric Research is sponsored by the National Science Foundation. The figures were prepared by Mr. Dewey L. Rudd. The author is also grateful to anonymous reviewers, whose comments greatly improved the clarity of the paper.

REFERENCES

Betts, A. K., 1976: The thermodynamic transformation of the tropical subcloud layer by precipitation and downdrafts. *J. Atmos. Sci.*, **33**, 1008–1020.

Burpee, R. W., 1972: The origin and structure of easterly waves in the lower troposphere of north Africa. *J. Atmos. Sci.*, **29**, 77–90.

——, 1974: Characteristics of north Africa easterly waves during the summers of 1968 and 1969. *J. Atmos. Sci.*, **31**, 1556–1570.

——, 1975: Some features of synoptic-scale waves based on compositing analysis of GATE data. *Mon. Wea. Rev.*, **103**, 921–925.

Carlson, T. N., 1969a: Synoptic histories of three African disturbances that developed into Atlantic hurricanes. *Mon. Wea. Rev.*, **97**, 256–276.

——, 1969b: Some remarks on African disturbances and their progress over the tropical Atlantic. *Mon. Wea. Rev.*, **97**, 716–726.

Chang, C. P., 1970: Westward propagating cloud patterns in the tropical Pacific as seen from time-composite satellite photographs. *J. Atmos. Sci.*, **27**, 133–138.

Dewart, J. M., 1977: Diurnal variations in the GATE region. Paper presented at U.S. GATE Central Program Workshop, NCAR, Boulder.

Frank, W. M., 1978: The life cycles of GATE convective systems. *J. Atmos. Sci.*, **35**, 1256–1264.

Gray, T. I., Jr., and A. H. Oort, 1974: Interannual variations in convective activity over the GATE area. *Bull. Amer. Meteor. Soc.*, **55**, 220–226.

Gray, W. M., and R. W. Jacobson, Jr., 1977: Diurnal variation of deep cumulus convection. *Mon. Wea. Rev.*, **105**, 1171–1188.

Gruber, A., 1972: Fluctuations in the position of the ITCZ in the Atlantic and Pacific Oceans. *J. Atmos. Sci.*, **29**, 193–197.

——, 1976: An estimate of the daily variation of cloudiness over the GATE A/B area. *Mon. Wea. Rev.*, **104**, 1036–1037.

Guillemin, E. A., 1957: *Synthesis of Passive Networks*. Wiley, 571 pp.

Hayashi, Y., 1977: Space-time power spectral analysis using the maximum entropy method. *J. Meteor. Soc. Japan*, **55**, 415–420.

Jury, E. I., 1964: *Theory and Application of Z-Transform Method*. Wiley, 624 pp.

Marks, R., 1975: Study of diurnal variation in convection using Quadra radar data—Phases I and II. GATE Rep. No. 14, WMO, 191–204.

McGarry, M. M., and R. J. Reed, 1978: Diurnal variations in convective activity and precipitation during Phases III and II of GATE. *Mon. Wea. Rev.*, **106**, 101–113.

Murakami, M., 1972: Intermediate-scale disturbances appearing in the ITC Zone in the tropical western Pacific. *J. Meteor. Soc. Japan*, **50**, 454–464.

Nitta, T., 1978: A diagnostic study of interaction of cumulus updraft and downdraft with large-scale motion in GATE. *J. Meteor. Soc. Japan*, **56**, 232–242.

O'Brien, J. J., 1970: Alternative solutions to the classical vertical velocity problem. *J. Appl. Meteor.*, **9**, 197–203.

Orlanski, I., 1976: The trapeze instability in an equatorial β-plane. *J. Atmos. Sci.*, **33**, 745–763.

——, and L. J. Polinsky, 1977: Spectral distribution of cloud cover over Africa. *J. Meteor. Soc. Japan*, **55**, 483–493.

Payne, S. W., and M. M. McGarry, 1977: The relationship of satellite infrared convective activity to easterly waves over west Africa and the adjacent ocean during Phase III of GATE. *Mon. Wea. Rev.*, **105**, 413–420.

Pedder, M. A., 1978: Diurnal and semidiurnal variations in the A/B scale-averaged wind fields during Phase III of GATE. *Mon. Wea. Rev.*, **106**, 782–788.

Reed, R. J., D. C. Norquist and E. E. Recker, 1977: The structure and properties of African wave disturbances as observed during Phase III of GATE. *Mon. Wea. Rev.*, **105**, 317–333.

Sadler, J. C., 1975: The monsoon circulation and cloudiness over the GATE area. *Mon. Wea. Rev.*, **103**, 369–387.

Shanks, J. L., 1967: Recursion filters for digital processing. *Geophysica*, **32**, 33–51.

Smith, E. A., and T. H. Vonder Haar, 1976: Hourly Synchronous Meteorological Satellite-1 (SMS-1) data collected during the GARP Atlantic Tropical Experiment (GATE). Tech. Note, Dept. of Atmos. Sci, Colorado State University, 180 pp.

Thompson, R. M., Jr., S. W. Phyne, E. E. Recker and R. J. Reed, 1979: Structure and properties of synoptic-scale wave disturbances in the Intertropical Convergence Zone of the eastern Atlantic. *J. Atmos. Sci.*, **36**, 53–72.

Zangvil, A., 1975: Temporal and spatial behavior of large-scale disturbances in tropical cloudiness deduced from satellite brightness data. *Mon. Wea. Rev.*, **103**, 904–920.

——, 1977: On the presentation and interpretation of spectra of large-scale disturbances. *Mon. Wea. Rev.*, **105**, 1469–1472.